Proudman Oceanographic Laboratory

Design and Laboratory Calibration of Piezoelectric Suspended Sediment Impact Probes

JJ Williams SP Moores PD Turney and KF Taylor
Report No. 46 1997

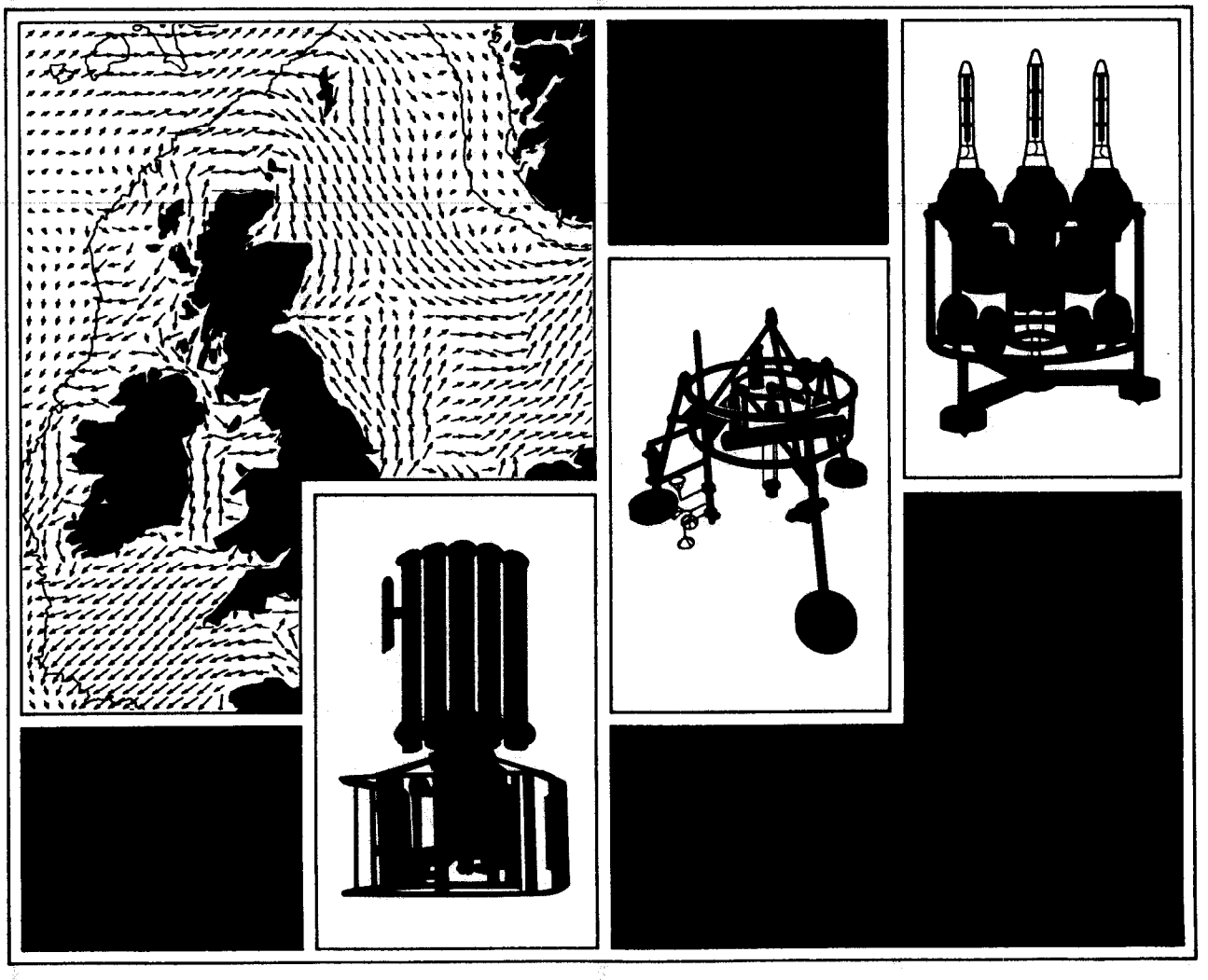

Natural Environment Research Council

PROUDMAN OCEANOGRAPHIC LABORATORY

Bidston Observatory
Birkenhead, Merseyside, L43 7RA, UK
Tel: 0151 653 8633
Telex: 628591 Ocean B
Fax: 0151 653 6269

Director: Dr. B.S. McCartney

Natural Environment Research Council

PROUDMAN OCEANOGRAPHIC LABORATORY

REPORT NUMBER 46

DESIGN AND LABORATORY CALIBRATION OF PIEZOELECTRIC SUSPENDED SEDIMENT IMPACT PROBES

J. J. Williams, S. P. Moores, P. D. Turney and K. F. Taylor

September 1997

DOCUMENT DATA SHEET

AUTHOR
WILLIAMS J. J., MOORES S. P., TURNEY P.D. &
TAYLOR K. F.

PUBLICATION DATE
1997

TITLE

Design and Laboratory Calibration of Piezoelectric Suspended Sediment Impact Probes

REFERENCE

Proudman Oceanographic Laboratory, Report No. **46**, 39pp.

ABSTRACT

The basic principles of piezoelectricity and the theories used in the application of this property to measuring the concentration of suspended sediment in the near-shore environment are reviewed. Information is given on the construction of a prototype suspended sediment impact probe (*SSIP-01*) which uses a piezoelectric ceramic to detect single grain impacts on a target. Electronic circuits built to control and improve the quality of the output signals from *SSIPs* are described and the construction of a vertical flume giving a homogeneous flux of suspended sediment for *SSIP* calibration are described. Methodologies used to calibrate *SSIPs* in the vertical flume are outlined and calibration results are presented. The design and fabrication of an improved *SSIP* instrument (*SSIP-02*) is presented and an assessment of instrument performance is given.

ISSUING ORGANISATION

Proudman Oceanographic Laboratory
Bidston Observatory
Birkenhead, Merseyside L43 7RA, UK

Acting Director: Dr J. M. Huthnance

TEL: ++ 44 51 653 8633
FAX: ++ 44 51 653 6269
TELEX: 628591 OCEAN BG

KEYWORDS

PIEZOELECTRICITY IMPACT PROBE
SUSPENDED SEDIMENTS

CONTRACT:
PROJECT: **MHT-49-5**
PRICE: £20.00

Contents

Contents

Page

Nomenclature

A	area
C	concentration of suspended sediment
D	grain diameter
D_{50}	median grain diameter
E	electric field (*volt/metre*)
I	grain impacts per minute
N	estimated number of sediment particles per kg
Q	charge
Q_s	sand injector discharge rate
S	strain
S_{tk}	Stokes number
T	stress
U	flow velocity
U_∞	free stream velocity
V	mean *SSIP* output voltage
Y	Young's modulus
c_1	piezoelectric constant (*Coulomb/Newton*)
c_2	piezoelectric constant (*volt/Joule*)
f_v	factor accounting for void spaces between packed grains
k	electromechanical coupling factor
l	*SSIP* target length
m	mass of a sand grain
m_m	momentum of impacting grain
t	target thickness
w	target width
μ	dynamic viscosity
ρ	fluid density
ρ_s	sediment density
σ_x	standard deviation

1.0 Introduction

In order to assess the feasibility of obtaining a continuous record of the concentration of suspended sand, *C*, in marine and fluvial situations, research has been undertaken in the past to assess the performance of various piezoelectric impact meters, (*Soulsby, 1977; Downing, 1981; Salkield et al. 1981*). In general, these instruments utilise a small ($1cm^2$ x 0.2mm) piezoelectric ceramic plate to convert the momentum of impacting sand grains into a voltage signal. In principle, a piezoelectric impact probe can be designed so that suspended particles with a density greater than water strike an impact target owing to their excess momentum and thereby impart mechanical energy to a piezoelectric ceramic. In contrast to active acoustic devices used to measure suspended sediment, impact devices are unaffected by air bubbles or low density particles entrapped in the fluid. Potentially, this makes them especially suited for measurements of suspended sediment concentration under conditions of breaking waves in the surf zone where air bubbles are usually present. Such an instrument may therefore allow quantification of on-offshore and along-shore sediment transport in the region of the coastal zone subject to the largest rates of suspended sediment transport and to the most rapid morphodynamic changes.

The relationship between suspended sediments in a flowing channel and impacts detected by piezoelectric sensors has been examined in past studies, (e.g. *Salkield et al. 1981*). Additionally, studies have been conducted into the relationship between suspended grain mass and piezoelectric output and the relationship between the number of detected grain impacts and the shape of the target. Analysis of various target designs has shown that employing a narrow rectangular target optimises the range of grain sizes and maximises the number of impacts for a given particle diameter. These laboratory studies have lead to the development of an existing sand transport probe, (STP, *Salkield et al. 1981*). Trial deployments of this instrument in the field are reported by *Soulsby et al., (1984; 1985).*

The four principle aims of the work presented here have been:

- to design and construct a vertical flume to provide a continuous circulating flow of water and suspended sediment in which a suspended sediment impact probe, *SSIP*, could be fixed and calibrated;
- to calibrate an existing *SSIP* design (*SSIP-01*) in controlled laboratory conditions;

- to design a new robust *SSIP* (*SSIP-02*) with improved signal:noise performance for use in near-shore environments; and
- to calibrate *SSIP-02* over an appropriate range of water velocities, U, grain sizes, D and sediment concentrations, C.

For testing and calibration purposes a range of sand grain diameters were chosen by considering the particle sizes found naturally in suspension in marine situations and the grain mass required to generate an impact response from the *SSIP*. Current velocities and sand grain diameters in the range 45cm/s to 70cm/s and 150μm to 300μm, respectively, were selected. Suspended sediment concentrations in the range 200mg/l to 900g/l were chosen as being representative of typical mean C values observed in coastal waters in current-only and wave-current conditions.

In the following sections the background pertaining to the operation and performance of *SSIPs* is presented and the *SSIP* calibration flume and calibration procedures are described. Results from the calibration of two *SSIPs* are presented and discussed and recommendations are given for future development work and applications.

2.0 Background

2.1 Piezoelectricity

The property of piezoelectricity can be defined as the interaction between electrical and kinetic energy within a material. When a piezoelectric material is subjected to a mechanical stress, an electrical field is generated which aligns dipoles within the material and produces a small potential difference across two of its faces. Additionally, the axis along which the electrical and mechanical effects take place within piezoelectric ceramics can be set relative to the principle axis of the ceramic shape by subjecting the material to a D.C. electric field and 'poling' it, (*Figure 1*), thereby making the material especially suited to a range of specialist applications. Further the ability to specify a wide range of sizes, shapes, physical characteristics and piezoelectric properties during manufacture makes piezoelectric ceramics very versatile materials.

When a material is subjected to a stress, T, the resultant strain, S, is found to be directly proportional and related by Young's modulus, Y, by the equation $T = Y\,S$. Piezoelectric materials additionally generate a charge density (coulomb/metre^2) perpendicular to the poling axis when subjected to a stress given by

$$\frac{Q}{A} = c_1\,T \qquad (1)$$

where c_1 is a piezoelectric constant (coulomb/Newton), Q is the resultant charge (coulomb) and A is the area perpendicular to the poling axis to which the charge is applied (m^2), (*Ikeda, 1990*). A second piezoelectric constant, c_2 (volt/joule) is used to relate an applied stress and the electric field, E (volt/meter) that is created along the poling axis (*Jaffe et al., 1971*) where

$$c_2 = \frac{E}{T} \qquad (2)$$

and hence,

$$T = \frac{Q}{c_1\,A} = \frac{E}{c_2} \qquad (3)$$

which shows that the resultant charge and electric field will increase proportionally with an increase in the applied stress. Alternatively, *Eq. 3* can be rearranged to give

$$E = c_2\,T = \frac{Q\,c_2}{c_1\,A} \qquad (4)$$

which indicates that a ceramic with a high value of c_2 and a low value of c_1 will generate larger output voltage signals. The efficiency of a piezoelectric material in converting mechanical to electrical energy is determined by the electromechanical coupling factor, k, where

$$k = \sqrt{\frac{\textit{mechanical energy converted into electrical energy}}{\textit{input mechanical energy}}}$$

The value of k cannot be greater than one since the mechanical to electrical conversion is always incomplete. The closer the value of k is to unity, the more versatile the piezoelectric material is. Research into the electromechanical coupling factor has shown that for quartz, barium titanate ceramic and lead zirconate titanate ceramic, k = 0.1, 0.4 and 0.5 to 0.7, respectively, which demonstrates that the lead zirconate titanate ceramic is the more suitable for detecting low stresses, such as those resulting from sand grain impacts on a target (*Jaffe et al., 1971*). Consequently, PZT5A[1] piezoelectric ceramic plates were used in the present SSIPs.

2.2 Impact and output signal relationships

The signal produced by a PZT5A piezoelectric ceramic when subjected to an applied stress can be detected by measuring the potential difference between each of the faces lying perpendicular to axis 3, (*Figure 1*). In the case of a sand grain striking a small, thin ceramic plate (1cm^2 x 0.2mm), the amplitude of the oscillating voltage signal caused by the impact decays to zero over a few hundred milliseconds with the decay period depending upon the operating mode of the ceramic, its piezoelectric properties and the magnitude of the impact, (e.g. *Figure 2*). Studies examining single grain and multiple grain impacts are reported by *Salkield et al, (1981)*. In the case of *SSIPs*, relationships between the magnitude of an impact and the output voltage signal have been calibrated for a number of different designs of *SSIPs* in the past and attempts have been made to relate the mean signal amplitude to the mean particle size and flux density of material passing the sensor, (*Salkield et al, 1981*).

The measurement of C in coastal waters can only be achieved if grains collide with the tip of the sensor. As suspended particles approach an *SSIP*, they are assumed to be moving with the same velocity and in the same direction as the fluid. If the density of an approaching particle (ρ_s) is much greater than that of the surrounding fluid then its momentum is also greater and hence the particle will continue approximately in a straight line and collide with the *SSIP*. Particles with a similar density to the fluid do not have sufficient excess momentum to strike the *SSIP* and may pass around it. The influence of the particle's density on its flow path can be exploited in the design of the target so that only particles with a density greater than a specific value will collide with an *SSIP*. This method of measuring suspended sediment concentration

[1] PZT5A are lead zirconate titanate ceramics with high sensitivity, permittivity and time stability. Present ceramic plates were supplied by Morgan Matroc Inc. (Fax: 01703 431768), UK. Full technical specification of PZT5A materials are given in Morgan Matroc (1996).

is particularly advantageous over non-impact techniques since most optical and acoustic methods require great care when attempting to distinguish between sand and other suspended materials in the water such as air bubbles, organic debris, clay and silt.

The size and shape of the *SSIP* is pivotal in determining the number of grain impacts detected by the piezoelectric ceramic. An increase in the area of the *SSIP* target exposed to the flow will theoretically increase the number of impacts but if the area exceeds a critical value, multiple impacts may occur. If the *SSIP* target area is increased still further, a region of turbulence is generated and the *SSIP* is likely to exhibit a non-linear response to changes in *C*. Consideration must also be given to the physical size and robustness of an *SSIP*.

3.0 *SSIP* signal processing

Typically, the output signal from the piezoelectric ceramic is spiky and contains significant background electrical noise. Tests undertaken have shown that signals resulting from grain impacts with the target are at least an order of magnitude larger than the background noise and can be easily distinguished. Electronic circuits designed to process raw output signals from *SSIPs* were designed here to perform two functions: (a) to count the number of grains impacting upon the target over a specified time period; and (b) to quantify the mean output voltage resulting from multiple grain impacts through time. Both these measurements were required subsequently to allow identification of the grain size in suspension at a given mean current speed and the concentration of suspended sediment present in the water at that speed.

The PZT5A piezoelectric ceramic material selected for use in the *SSIPs* gave a response signal to a single impact lasting of the order 100ms and damping to zero within several wavelengths at the resonant frequency of the ceramic, $\approx$ 150kHz, (e.g. *Figure 2*). Signals resulting from grain impacts were passed through three op-amps with a combined gain of 81dB, (*Figure 3*). The voltage response required further refinement to ensure that only signals within the ceramic response frequency range proceeded through to the next signal processing stage. This was achieved by passing the signal through a band pass filter set with a high pass of 100kHz and a low pass of 200kHz.

The number of impacts detected by the target were recorded using a comparator and a counter display, (*Figure 4*). A potentiometer was used to set a reference voltage level at one comparator input and when this was equalled or exceeded by the input voltage signal from the *SSIP* at the second input, the comparator output changed state from a one to a zero or vice versa which in turn updated the count display by one. The circuit was capable of counting grain impacts at a maximum rate of 10kHz and up to a maximum value of 999,999 before being reset. A half wave signal rectifier was used to convert the alternating voltage signal from the band pass filter into a direct positive signal, (*Figure 5*). This enabled the mean positive voltage signal amplitude to be calculated which was related in theory to the impacting grain diameter and the grain velocity.

An envelope detector circuit, (*Figure 6*), was then used after the rectifier to produce a voltage level that approximately 'enveloped' the peaks of the grain impact signals. The duration over which the signal envelope decayed was controlled by varying the value of the resistors. By using low value resistors, the output voltage level closely resembled the signal entering the envelope detector and hence produced unsatisfactory results. Conversely, use of high value resistors resulted in the capacitor charging and discharging at a much slower rate and hence produced a voltage level that fluctuated at a very low rate. Resistor values were therefore chosen that optimised circuit performance over a range of *SSIP* input levels.

The output from the envelope detector was passed through an analogue to digital converter (ADC) and logged at 20Hz on a PC. The maximum input voltage that the ADC was capable of converting was 5V and hence a non-inverting amplifier was introduced after the envelope detector circuit to attenuate or enlarge the greatest signal to approximately 4.5V. A flow diagram of the electronic circuits utilised in the present *SSIP* design and schematic representation of typical input and output signals at various stages in the signal processing procedure is given in *Figure 7*.

4.0 Vertical calibration flume

4.1 Flume design

In order to calibrate *SSIPs*, it was necessary to design a special flume with a working section through which a steady and reproducible flow of water could circulate. In addition a

device to introduce a constant supply of sand into the flow was required and a method by which to efficiently mix the sediment to produce a homogeneous suspension of sediment was needed. Conventionally, calibration of optical and acoustic devices to measure C is undertaken in turbulent channel flow or in an agitated settling tower. In many cases the concentration of suspended sediment in these facilities may be characterised by a vertical gradient owing to the effects of gravity or to inefficient mixing and thus a homogeneous suspension of sediment required for calibration purposes may not be achieved. In the present study this problem has been overcome through use of a purpose built vertical flume which mixes sediment and water effectively and eliminates stratification effects.

The vertical flume, *Figure 8*, consists of three connected tanks which allow water to circulate though a vertical working section using a submersible pump[2]. *Tank A* is used as a reservoir into which water can be pumped to provide a constant head of water above the working section. Flow into and out of *tank A* is regulated by overflow pipes. *Tank B* is used as a container into which the discharge from the vertical working section of the flume can settle and before passing over a weir and into *tank C* where the pump delivers water back to *tank A* at a rate of up to 17 litres per second. The rate of discharge from the pump was regulated by an adjustable valve.

To ensure that a homogeneous flux of suspended sediment entered the working section, the water flowing into the vertical flume required a high degree of mixing. This was achieved through use of an in-line *static mixer*[3] fixed directly above the working section of the flume. This device consists of a series of helical blades to generate turbulence and mix rapidly the sediment with the water to produce a uniform concentration of suspended material across the exit cross-section. Once mixed, large scale turbulent fluid motion was removed as the flow passed through a number of 10mm diameter tubes fixed together in a 'honeycomb' to fill the cross sectional area of the flume beneath the exit from the *static mixer*. To reduce flow turbulence above the static mixer, a brass mesh and vertical baffles were installed above the inlet. This ensured that sediments entering the mixer *(see below)* were not dispersed into *tank A*.

---

[2] Flygt 215 centrifugal, c/w 3kW 415/3/50 motor (tel: 01602 614444)

[3] Chemineer model 4-KME-PVC-2 (tel: 01332 363175)

4.2 Sand injector

In order to introduce sand into the circulating water system, a device was required that was capable of providing a steady discharge of sand spanning a range of required sediment flow rates. The sand injector device designed consisted of a Perspex hopper with a funnelled base positioned over a horizontal stainless steel pipe into which sand fell under gravity from the hopper, (*Figure 9*). Compressed air was passed through the pipe using a regulator to adjust the supply pressure. The resulting air and sand mixture was then discharged through a 90° curved pipe which propelled sand into the water above the inlet to the working section of the flume. An adjustable valve on the base of the hopper was used to vary the size of the opening through which the sand fell and the angle at which the sand passed into the pipe, (*Figure 9*). The compressed air supply to the injector also generated a venturi effect beneath the bottom of the sand hopper which actively improved the flow of sand.

The injector was calibrated over a range of air pressures and then fixed above *tank A* such that the outlet nozzle was positioned directly above the centre of the static mixer at a distance from the water surface which prevented excessive splashing at the maximum air pressure used to inject the sediment. In order to prevent recirculation of the injected sand and to enable the mass of sand passing down the flume to be calculated, a 100μm mesh net was attached to the flume outlet (*Figure 8*). A stainless steel hoop was fitted into the inlet of the sampling net to maintain the shape of the opening. The hoop was suspended by nylon chords around the flume at a height so as not interfere with the flume discharge and ensure collection of all sediment exiting the working section.

The sand injector was calibrated to allow the operator to control accurately the mass of sand discharged from the outlet nozzle per second and hence permit precise control over the amount of sand entering the vertical flume. Beach sand was collected from the north Wirral coastline and sieved into grain diameter ranges of 150μm-180μm, 180μm-212μm, 212μm-250μm and 250μm-300μm using a stacked sieve vibrator and British Standard sieves. Median grain diameters (D_{50}) for each size range was 165μm, 196μm, 231μm and 275μm, respectively.

Initially, the discharge of sand from the injector outlet was obstructed by moist sand particles causing them to bond together and block the hopper valve. To overcome this problem

the injector was set at a suitable distance above the water surface and an in-line moisture remover comprising a silica gel cartridge was introduced to the air line. In addition a device to vibrate the hopper was also fitted to the sand injector system. During initial tests the sand injector was set up on a horizontal surface with the air line pressure regulator set at 0.4bar. A volume of 250-300μm sand was poured into the hopper, the vibrator was switched on and the sand discharged freely into a collection bag. Once a constant flow of sand had been achieved, a pre-weighed net was placed over the nozzle for one minute and then re-weighed to determine the discharge rate of the injector in grams per minute. This procedure was repeated a further four times at the same pressure and then again at pressures ranging from 0.6 to 1.4bar increasing in 0.2bar increments. The injector was calibrated with the three remaining grain diameter ranges and the mean and standard deviation of sediment discharge rates were calculated (*Table 1*).

	Grain diameter (μm)							
	250 - 300		**212 - 250**		**180 - 212**		**150 - 180**	
Pressure (bar)	Mean	σ_x	Mean	σ_x	Mean	σ_x	Mean	σ_x
0.4	*49.6*	*1.2*	*52.4*	*1.4*	*53.6*	*1.2*	*53.0*	*1.3*
0.6	*51.6*	*1.3*	*55.0*	*1.2*	*54.6*	*0.9*	*50.8*	*0.7*
0.8	*58.5*	*0.9*	*59.4*	*1.2*	*57.0*	*0.9*	*53.0*	*1.2*
1.0	*63.2*	*0.8*	*63.3*	*0.8*	*60.0*	*1.2*	*55.6*	*1.6*
1.2	*67.5*	*1.6*	*66.5*	*1.7*	*62.6*	*1.5*	*58.4*	*0.9*
1.4	*70.8*	*1.1*	*69.2*	*1.3*	*65.9*	*1.4*	*62.1*	*1.2*

Table 1 Mean and standard deviation, σ_x, of the sand injector discharge rate, Q_s (g/min)

Table 1 shows that σ_x for any given grain size or sand injection pressure is of the order of 2% of the mean demonstrating that a reproducable and steady discharge of sand can be achieved using the sand injector. Sediment collected in the net beneath the working section of the flume also confirmed that the mass of sediment present in the flow over a fixed period of time was also constant and reproducable.

4.3 Flow in the working section

Measurements of water velocity were obtained using a *Nixon low-speed Streamflo*[4] current meter (*Series 403B, 5cm/s to 150cm/s*), (*Figure 10; Appendix 1*). All tests showed that reproducible flow velocities could be achieved in the working section. In addition, at distances more than 1cm from the side wall of the working section a uniform flow velocity was measured at locations spanning the diameter of the working section irrespective of the mean flow velocity. Further details of velocity profiles in the working section are given in *Appendix 1*.

4.4 Sediment sampler

In order to determine the degree of homogeneity in the flux of suspended sediment, a device was required to measure suspended sediment concentrations at spanwise locations in the working section of the flume. The sampler designed for these tests was positioned in the working section and consisted of a copper pipe with a vertical inlet that followed a gentle curve into a horizontal section. This was then connected to a flexible hose through which water and sediment from the working section could flow, (*Figure 11*). Flow in the sampler was sufficient to ensure sand did not settle whilst in transit between the working section of the flume and the sediment/water collection point.

Sediment sampling was undertaken using the sampler, *Figure 11,* to determine values for C in the working section of the flume during calibration runs. During initial tests, the sampler was positioned in the flume at different spanwise locations. The flow rate through the sampler was calculated a number of times to check that it was reproducible and to determine the difference between the velocity in the flume and in the sampler. For a given sampler position in the working section the sampler outlet was placed inside the capture net at the base of the flume and the sand injector air line pressure was increased to 1.0 bar. The apparatus was left for approximately 5 minutes to stabilise. Values for C were determined by placing a net over the sampler outlet and collecting sand for a timed duration. The measured mass of retained sand (mg), the sampler discharge rate (l/s) and the sample duration (s) were then used to calculated the sediment concentration (mg/l) in the working section. This procedure was repeated a further four times and then again at 10mm intervals across the flume diameter.

---

[4] Nixon Instrumentation (Fax: 01242 222487)

This method of sediment sampling described above allowed collection of a large quantity of sand with no limitations due to time or the volume of water discharged by the sampler. The lowest standard deviation for C occurred at the centre of the flume, thus making this an ideal location for calibration of an *SSIP*. Measured spanwise variation in C values were low irrespective of the selected flow velocity or sediment grain size. Results from this investigation are given in detail in *Appendix 2*.

5.0 *SSIP* calibration and performance

The following sections describe the calibration procedure used to determine the relationship between *SSIP* output and C over a range of selected flow velocities. In the first series of tests an impact probe based upon the design by *Salkield et al., (1981)*, *SSIP-01*, was used, (*see Appendix 3a*). The performance of this prototype instrument was not found to be satisfactory and an alternative *SSIP* design was sought. The design, construction, calibration of the new *SSIP* instrument, *SSIP-02*, giving enhanced performance of a wide range of grain sizes is detailed in *Appendix 3b.*

5.1 *SSIP-01* testing and calibration

SSIP-01 was positioned in the centre of the working section of the vertical flume, (*Figure 8).* During initial trails it was observed that sand grains tended to follow flow streamlines and were diverted away from the target at working section flow velocities above 70cm/s. As a result grain impact counts were much lower than expected, *Appendix 4.* At velocities lower than 40cm/s, sand grains striking *SSIP-01* had insufficient momentum to generate an impact voltage above the background noise level associated with this instrument. Thus the test flow velocities chosen for calibration of *SSIP-01* lay between these two values.

In order to determine the background or 'zero-offset' characteristics of *SSIP-01*, the output from the envelope detector was recorded for 40 seconds without sediment present in the flow. The water velocity just above *SSIP-01* was measured using the flow meter, (*Appendix 1*). Sand was then injected into the flume at a pressure of 1bar and two records of the envelope detector output and the number of impacts detected by the *SSIP-01* were obtained. Following these measurements a second zero-offset run was carried out. The sand injector, flume and collection net at the flume outlet were thoroughly cleaned to remove all sand grains and the

measurements described above were repeated. The same calibration procedure was applied using the range of selected test sediments, (i.e. D_{50} = 165μm, 196μm, 231μm and 275μm), and flow velocities in the range 45cm/s to 65cm/s. By altering the pressure of the air supply to the sand injector, C values in the range 200mg/l to 900mg/l were obtained.

Figure 12 show the measured relationship between: *(a)* the mean *SSIP-01* output voltage and D_{50}; and *(b)* the normalised *SSIP-01* output, expressed in units of mV/impact, and D_{50} over the flow velocity range 45cm/s - 65cm/s. *Figure 12a* shows that the expected linear relationship between *SSIP-01* output and D_{50} is only measured for flow velocities of 65cm/s. The remainder of the plots deviate from a straight line and show little discrimination between grain sizes at a given flow velocity. *Figure 12b* also shows that *SSIP-01* cannot discriminate clearly between different grain sizes. It was also found that the relationship between the mean *SSIP-01* signal and C and between the number of grain impacts per minute (I) detected by *SSIP-01* and C were unclear and failed to discriminate between different test grain sizes *(not illustrated)*.

These results suggests strongly that the grain detection efficiency of *SSIP-01* is a non-linear function of the flow velocity and indicates, therefore, that the hydrodynamic shape of *SSIP-01* is less than ideal. *Figure 12a* shows clearly that the output voltage from *SSIP-01* does not conform to the expected theoretical trends. Further, irrespective of grain size, the number of grain impacts measured during a one minute period were of the order of 0.5% of the expected number (*Appendix 4*). It is considered that at low flow velocities, most of the suspended sand grains possessed insufficient momentum to strike the *SSIP* and thus the mean output voltage is similar for the range of grain sizes and working section velocities examined. At higher flow velocities, grains simply diverged away from the target shortly before impact and were not detected by *SSIP-01*. In addition, it was also observed that at certain combinations of working section flow velocities and grain sizes, a number of the impacts recorded by the counter circuit were the result of sand grains colliding with the main body of the probe which resulted is spurious results. Having obtained these first calibration results the performance of *SSIP-01* was considered to be unsatisfactory and an alternative *SSIP* design was developed and further calibration tests using *SSIP-01* were suspended.

5.2 *SSIP-02* testing and calibration

Since the performance of the *SSIP-01* design depends critically upon the shape of the instrument and the efficiency of the mechanical coupling between the target and the piezoelectric ceramic, (*Appendix 3a*), and this was probably less than ideal in the present design, a second design approach utilised an epoxy resin containing stainless steel particles to manufacture an integral impact surface and detector unit. Full details of the fabrication of the new impact probe (*SSIP-02*) are given in *Appendix 3b*.

During initial trails of *SSIP-02* the number of impacts recorded were found to increase with velocity even though the sand injector discharge rate remained constant. This was caused by secondary oscillations of the piezoelectric ceramic, (*Figure 2*), which in some instances were large enough to trigger the counter circuit. To overcome this problem a non-retriggerable monostable was introduced to the counter circuit after the comparator. Any secondary pulses were then ignored when the monostable was set to remain either high or low for the oscillating signal duration ($\approx$ 100μs, *Figure 2*). Following this modification initial tests showed the background noise level of the *SSIP-02* was an order of magnitude less than the background noise level of *SSIP-01* and that the output from the *SSIP-02* instrument for a given grain impact was an order of magnitude larger than that resulting from comparable impacts recorded using *SSIP-01*.

The calibration procedure applied for *SSIP-02* followed the same routine as that used for *SSIP-01*. Tests were conducted using 'fine' sediment (150μm to 180μm) and 'coarse' sediments (250μm to 300μm) at working section flow velocities, U, of $\approx$ 45cm/s, $\approx$ 57cm/s and $\approx$ 70cm/s. Sediment concentrations ranged between 200g/l and 900g/l in all test cases examined. During each calibration run the background output voltage measured using the envelope detector and the number of grain impacts per minute were recorded.

Results from the calibration tests obtained using *SSIP-02* are presented in *Figure 13* (150μm to 180μm) and *Figure 14* (250μm to 3000μm). In *Figure 13*, for convenience, the relationship between the mean *SSIP-02* output (V) and C for U = $\approx$ 45cm/s, $\approx$ 57cm/s and $\approx$ 70cm/s is shown using log-linear axes. Each one of these three curves is shown in detail in *Figures 13b*, *Figure 13c* and *Figure 13d* which also show a least-squares linear regression

between *V* and *C*. In *Figure 13e*, for convenience, the relationship between the number of grain impacts detected per minute by *SSIP-02* (*I*) and *C* for *U* = ≈ 45cm/s, ≈ 57cm/s and ≈ 70cm/s are also shown using log-linear axes. Plots showing a least-squares linear regression between *I* and *C* are given in *Figures 13f* to *13h*. Results of the *SSIP-02* calibration using the 250μm to 300μm sediment are presented in the same way in *Figure 14*.

Figure 13 and *Figure 14* show clearly the enhanced performance of *SSIP-02* over the range of grain sizes and flow velocities tested. As expected from theoretical considerations a linear relationship between *V* and *C* and between *I* and *C* is obtained in all cases ($R^2 > 0.89$). *Figure 13* and *Figure 14,* showing that maximum *V* values for the 250μm to 300μm sediment are a factor of ≈3.3 times larger than *V* values for the 150μm to 180μm sediment illustrate that it is also now possible to discriminate between different grain sizes using *SSIP-02*.

However, whilst *Figure 13* and *Figure 14* show a linear relationship between *V* and *C* and between *I* and *C* for the range of grain sizes and flow velocities tested, the observed number of grain impacts per minute do not conform to expected values (*Appendix 4). Figure 15a* shows the relationship between *I* and *C* for observed (*SSIP-02*) and calculated values of *I* for 150μm to 180μm sand over the *U* range ≈ 45cm/s to ≈ 70cm/s. It is clear that *SSIP-02* fails to detect > 90% of the 150μm to 180μm grains in suspension. However, for the 250μm to 300μm sand *Figure 15b* shows a much closer agreement between observed and calculated *I* values. For *U* values > 45cm/s, observed and calculated *I* values follow the same trend and differ by approximately 30% thus indicating that the sampling efficiency of the *SSIP* target is relatively high.

In a final series of tests, the response of *SSIP-02* to entrapped air bubbles and fine sediments was tested. A continuous stream of fine air bubbles was injected in the working section of the flume using the sand injector and were carried by the flow past *SSIP-02*. No change in the 'background' count rate or in the mean output voltage was detected. Similarly, the presense of fine sediments, (D_{50} ≈ 30μm), in concentrations up to 2000mg/l were not detected by *SSIP-02*.

In conclusion, results presented above have shown that it is now possible to measure C provided an independent measurement of U and D are also obtained. Since the efficiency of the *SSIP* target in detecting grains is a function of U, D and the physical size and shape of the target, further work is now required to optimise target design for a given application. The importance of this measurement technique for measuring suspended sediments in nearshore environments cannot be over stressed and further development work on *SSIPs* is strongly recommended.

6. 0 Summary

A vertical flume for the calibration of *SSIPs* has been designed, constructed and tested. Devices to produce a homogeneous and reproducible concentration of suspended sediment in the working section have been devised and a simple, accurate sediment sampling system developed. Calibration tests have been undertaken using two *SSIP* designs using a range of natural sediment grains with median grain diameters of 165μm, 196μm, 231μm and 275μm over the flow velocity range 45cm/s to 70cm/s and the suspended sediment concentration range 200mg/l to 900mg/l. *SSIP-01* was found not to perform well owing to design and construction flaws. The output signal from *SSIP-02* followed theoretical expectations and allowed measurement of C and D_{50}. By virtue of *SSIP-02* design, spurious sensor response to bubbles, silt/clay or material of biological origin is negligible. Whilst the design of an optimum *SSIP* target for a given application required further work, the present study has proven the concept of using piezoelectric sensors to measure C in a range of different flow condition and over a range of different grain sizes. The *SSIP* has the potential to be an effective instrument for use in the surf zone and other marine locations where entrapped air bubbles preclude the use of active acoustic sensors. The instrument has potential applications in a number of existing and future *POL*[5] projects and may provide information from environments where existing instrumentation simply does not work. Further investment of research effort is required to bring the concept to fruition.

7.0 Recommendations for further research

Over the limited range of flow velocities and sediment grain sizes studied, *SSIP-02* has enabled the measurement of suspended sediment concentration and the discrimination of

[5] Proudman Oceanographic Laboratory

particle size. However, the grain impact detection efficiency is < 100% of the expected number of impacts in a given suspended sediment concentration and it is considered that the present design can be refined further by investigating the relationship between target shape and size and the grain impact detection efficiency. Impact signal degradation and electrical noise levels may be reduced further through use of a pre-amplification circuit close to the piezoelectric ceramic. This unit could be incorporated into the main body of the *SSIP*. The use of a log-response operational amplifier is also advocated in future designs. Further studies should be conducted in order to identify the optimum piezoelectric material for the present application. It is considered that with the assistance of an electronic engineer these improvements of *SSIP* performance could be achieved.

With further laboratory development of the *SSIP* completed the instrument requires field trials in current-only and wave-current situations. It is recommended that in the current-only case the *SSIP* be deployed on a bottom mounted frame in conjunction with an acoustic backscatter probe, *ABS*, pump-sampling and an acoustic Doppler velocimeter, *ADV*. All instrumentation requires cables to the shore for data logging/sample collection purposes. Suitable locations in the upper reaches of the Dee estuary ($D_{50} \approx 300\mu m$; $U \approx 2m/s$) have been identified for these tests.

In wave-current conditions, a critical test of instrument performance concerns the measurement of suspended sediment concentrations in the breaker zone. It is suggested that again a bottom mounted frame is used to deploy the *SSIP* and pump sampling equipment. Since *ABS* instruments cannot be used in this situation, and the performance of *ADV*'s has not been tested in breaking and shoaling wave conditions, consideration must be given to the most suitable instrumentation for measurement of current velocity. Following more detailed laboratory work relating grain impact magnitude to flow velocity it might be possible to rely upon the mean output level from the *SSIP* as a surrogate measure of flow velocity if the grain size distribution present at the field site is uniform and narrow.

Acknowledgements

The authors wish to express their thanks to Roger J. Williams at *BNFL*[6] for his contribution to the design of the vertical flume apparatus. The work was funded jointly by the Natural Environment Research Council and by the Flood and Coastal Defence Division of MAFF.

References

DOWNING, J. P. (1981) Particle counter for sediment transport studies. *Journal of the Hydraulics Division, American Society of Civil Engineers*, **107** (*HY11*), 1455-1465.

IKEDA, T. (1990), *Fundamentals of Piezoelectricity* , Oxford Science Publications.

JAFFE, B., COOK, W. R. & JAFFE, H. (1971), *Piezoelectric Ceramics*, Academic Press Inc. Ltd.

MORGAN MATROC INC. (1996) *Guide to modern piezoelectric ceramics*. Morgan Matroc Inc. UK, 27pp.

SALKIELD, A. P., LEGOOD, G. P. & SOULSBY, R. L. (1981) An Impact Sensor for Measuring Suspended Sand Concentration. Reprinted from the Paper Presented at the *Conference on Electronics for Ocean Technology*, Birmingham, UK, 12pp.

SOULSBY, R.L. (1977) Sensors for the Measurement of Sand in Suspension, *Institute of Oceanographic Sciences,* Report No **27**, Taunton, England, 48pp.

SOULSBY, R. L., SALKIELD, A. P. & LE GOOD, G. P. (1984) Measurements of the turbulence characteristics of sand suspended by a tidal current. *Continental Shelf Research*, **3**(4), 439-454.

SOULSBY, R. L., SALKIELD, A. P., HAINE R. A. & WAINWRIGHT B. (1985) Observations of the turbulent fluxes of suspended sand near the sea-bed. *Proceedings Euromech* **192**, D11, 7pp.

[6] British Nuclear Fuels Limited

Appendix 1 Working section velocity profiles

A *Nixon Streamflo* current meter (*Series 403*) with a diameter of approximately 1cm was used to measure flow velocity at spanwise locations across the working section of the flume. The output frequency of the instrument is related to the water velocity by the calibration

$$Velocity(cm/s) = \frac{Frequency\ (Hz) + 2.324324}{0.4108108}. \qquad (A1.1)$$

By passing the current meter output signal through a *current to voltage* converter, the signal could be logged using a PC. The converted voltage signal from the current meter was calibrated by placing the current meter probe in a low turbulence, continuous flow of water and adjusting the rate of discharge until a reading of 10Hz was shown on the frequency display. The signal was logged for 60-s and the process was repeated at 20Hz, 30Hz and 40Hz. Measurements confirmed a linear relationship between flow velocity (U) and the mean output voltage level (V) expressed as

$$U = -2.241 \times 10^{-2}\ V + 5.658 \qquad (A1.2)$$

The flow meter probe was used to measure flow velocity across the diameter of the flume at distances z from the side wall of the working section. Results of this study are presented in *Table A1.1* and *Figure A1.1* and demonstrate flow uniformity across the majority of the working section of the *SSIP* calibration flume.

z (mm)	U (cm/s)		
	High	**Medium**	**Low**
10	*87.8*	*61.6*	*39.7*
20	*88.4*	*64.1*	*37.3*
30	*83.6*	*59.2*	*34.9*
40	*79.3*	*56.8*	*32.4*
50	*78.1*	*56.8*	*33.7*
60	*78.7*	*58.0*	*33.7*
70	*82.9*	*58.0*	*34.9*
80	*84.2*	*60.4*	*34.9*
90	*82.9*	*59.2*	*33.7*
100	*80.5*	*58.0*	*29.4*

Table A1.1 Observed flow velocity at locations across the working section of the *SSIP* calibration flume

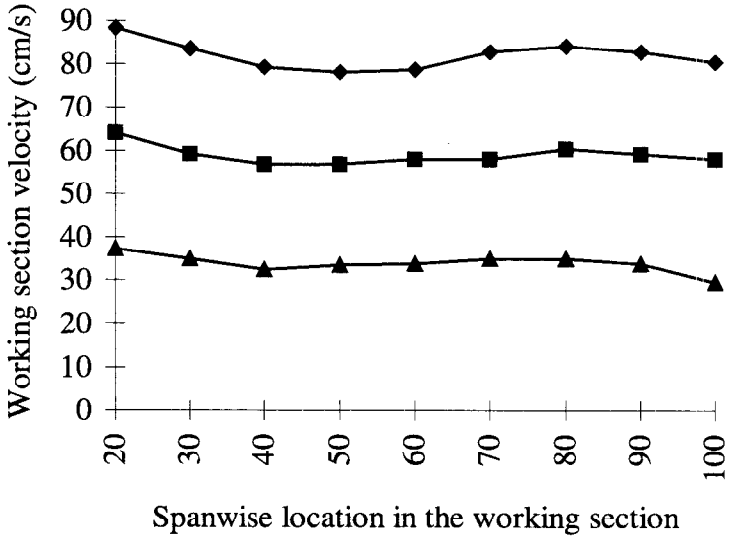

Figure A1.1 Spanwise variation in working section velocity

Appendix 2 Working section suspended sediment concentration profiles

The following suspended sediment concentration values, C, and standard deviation values for C, σ_s, were measured using the sediment sampler described in 4.4. Selected results of this study, presented in *Table A2*, confirm a uniform distribution of suspended sediment concentration across the width of the working section of the *SSIP* calibration device. Similar results were obtained for other C and U values.

z (mm)	C (mg/l)	σ_s (mg/l)	C (mg/l)	σ_s (mg/l)	C (mg/l)	σ_s (mg/l)
20	*134*	*8*	*274*	*10*	*482*	*16*
30	*147*	*7*	*269*	*11*	*493*	*18*
40	*126*	*4*	*276*	*9*	*496*	*17*
50	*146*	*4*	*282*	*9*	*473*	*15*
60	*126*	*5*	*265*	*10*	*481*	*14*
70	*124*	*8*	*269*	*12*	*499*	*19*
80	*127*	*4*	*271*	*8*	*475*	*16*
90	*123*	*6*	*273*	*10*	*486*	*15*

Table A2.1 Observed suspended sediment concentration, C and standard deviation of C, σ_s, at locations, z, across the working section of the *SSIP* calibration flume for U = 55cm/s

Appendix 3a Fabrication of SSIP-01

An *SSIP* (*SSIP-01*), similar in design to that reported by *Salkield et al, (1981)* was constructed by sandwiching a PZT5A piezoelectric ceramic plate (1cm x 1cm x 0.2mm), a stainless steel tip and a length of glass epoxy laminate board between two stainless steel plates to shield the ceramic from electrical noise, (*Figure A3.1*). The output signal wires were connected to the ceramic plate using the method described in *Appendix 3b* and were connected to a length of screened coax cable. The instrument was then sealed in an epoxy resin to form the body of the *SSIP-01* design. The stainless steel tip was place against the end face of the piezoelectric plate to preserve its piezoelectric properties by reducing the magnitude of grain impacts and to insulate the *SSIP* from electrical noise.

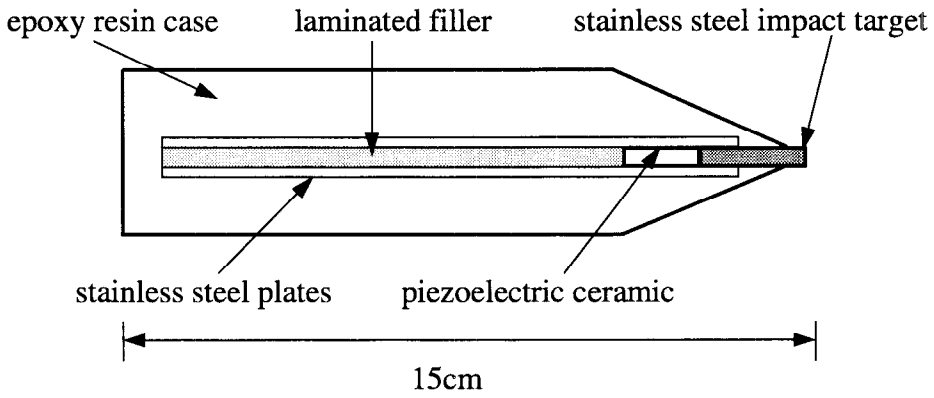

Figure A3.1 Side view of *SSIP-01*

Appendix 3b Fabrication of SSIP-02

Contacts to each face of the piezoelectric ceramic plate were made using *40 SWG* lacquered copper wire. The wires were dipped in ethanol and tinned before being soldered to the silvered faces of the ceramic plate using 2% silver solder. To avoid damage to the ceramic, care was taken to ensure that the soldering iron temperature did not exceed the Curie temperature (*i.e.* < 300°). An insulating varnish was then applied to the ceramic and the wires to prevent contact between the ceramic and the stainless steel/epoxy resin in the subsequent assembly stages. A streamlined profile for the leading edge of *SSIP-02* was designed using the curve

$$y = t\left[1 - \left(\frac{x}{l}\right)^3\right]^{\frac{1}{2}} \qquad (A3.1)$$

where t is required thickness of the target, y is the distance from zero along the y-axis, x is the distance from zero along x-axis and l is the required length of the target. In the present case a curve with thickness 1mm and length 13mm promotes the smooth development of a boundary layer and inhibits flow separation until well beyond the leading edge over the range of Reynolds numbers for the calibration tests.

A mould conforming to the required target shape was manufactured and the ceramic plate and electrical contacts were placed in the required position within the body of the mould. To ensure electrical isolation from the stainless steel/epoxy resin, the ceramic plate was encased in thin card and sealed using self-amalgamating tape (*Figure A3.2*). The stainless steel/epoxy resin was then poured into the mould and was subjected to a reduced pressure to aid the removal of entrapped air bubbles. When cured, the moulding was removed and smoothed using fine grade *wet & dry* paper. The moulding was than held in a rigid *PVC* holder and the two electrical leads from the encased ceramic were connected to a screened coax cable. Rubber strips were used to fill the small gap between the target tip and the *PVC* body to ensure that the target head was securely fixed in place and isolate from the rigid *PVC* body.

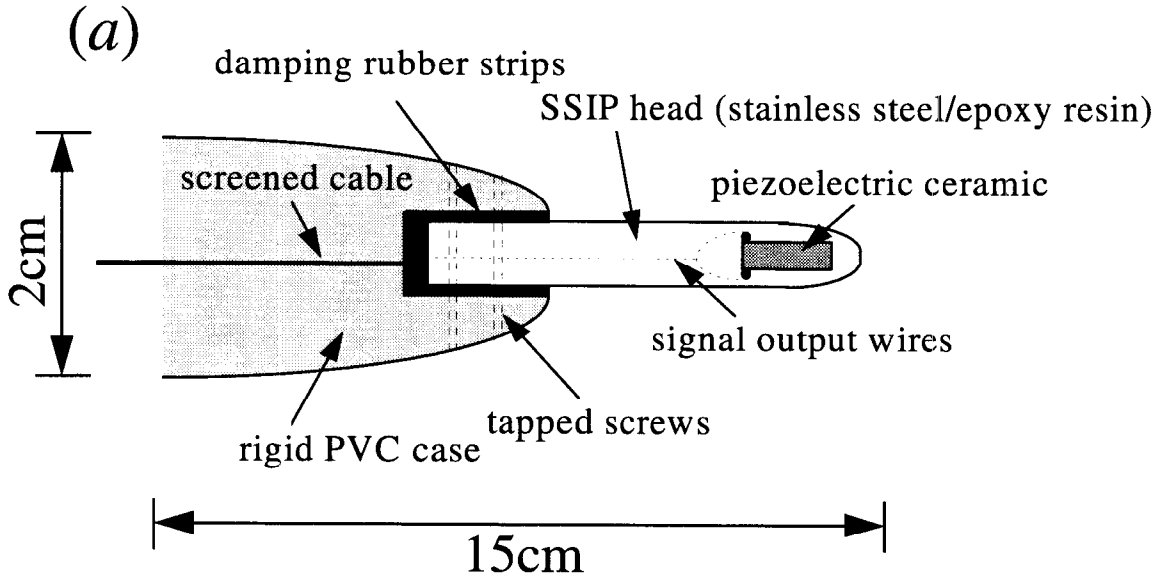

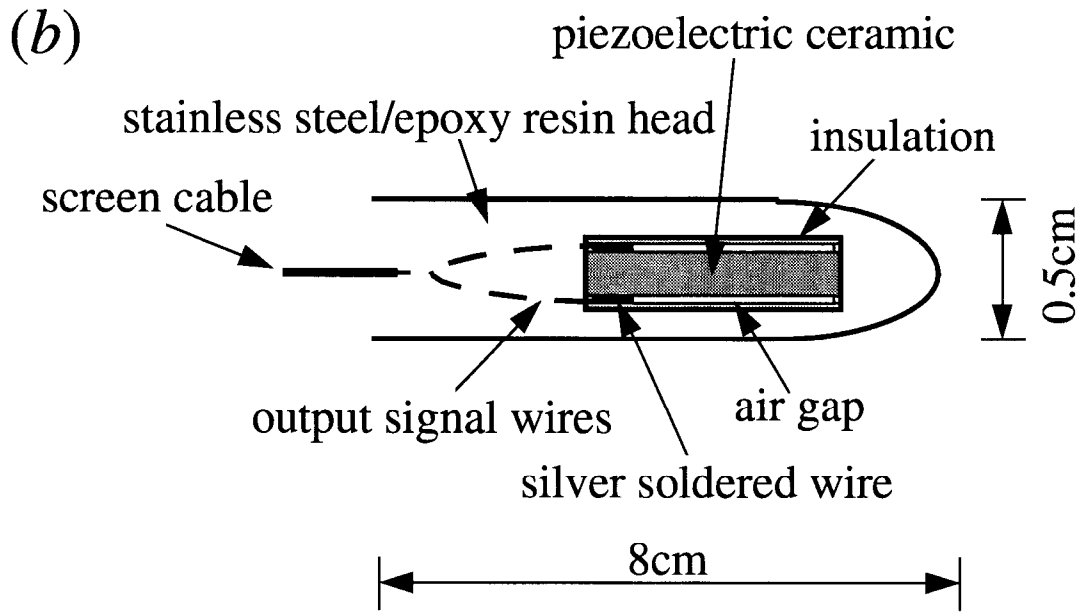

Figure A3.2 (*a*) Side view of *SSIP-02*; and (*b*) details of the ceramic plate emplaced in the stainless steel/epoxy resin target tip.

Appendix 4 Expected number of grain impacts

The theoretical number of impacts experienced by an *SSIP* target per second was calculated as follows: the mass of single sand grain, m (kg) = *Volume* (m^3) * *Density* (kg/m^3) thus: $m = 4/3\pi\ r^3.2650$, where r is the radius of sand grains (m). It was assumed that the number of particles per kg, $N = (1/m) - f_v$, where f_v is a factor to account for void spaces between grains. Here it was assumed that f_v = 10% of the total volume. Thus for a given suspended sediment concentration (kg/m^3) the theoretical number of grain impacts per second, N_i, upon a target area A at flow velocity U is given by $N_i = U.C.A\ N$. Results of these calculations are shown in *Figure 15*.

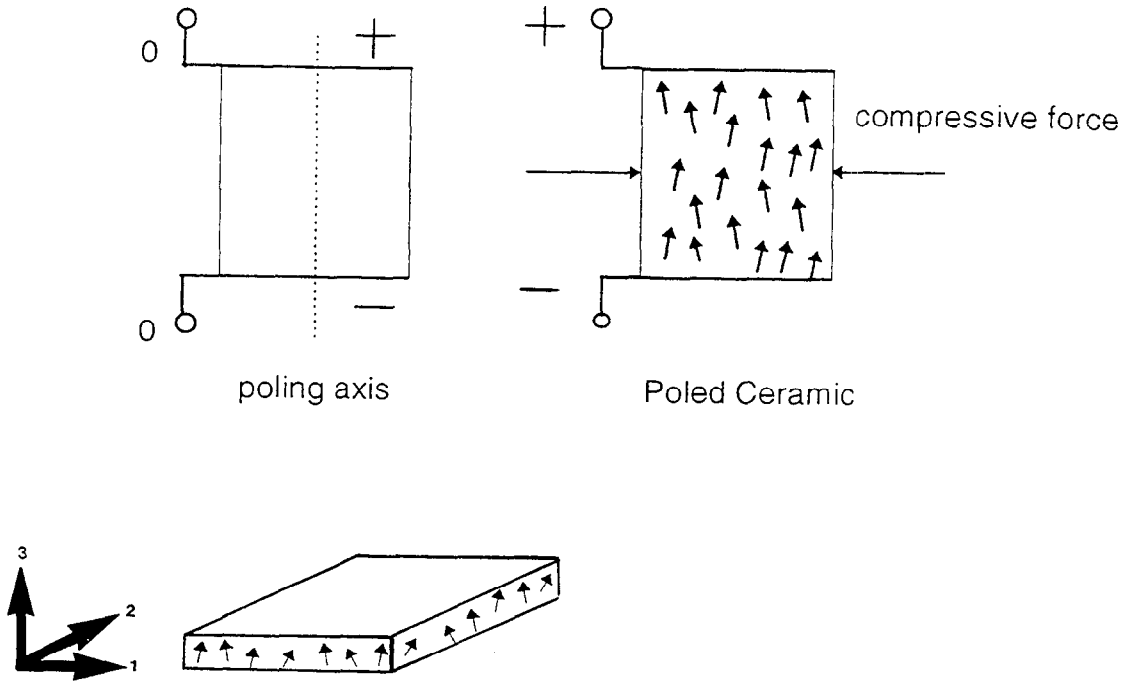

Figure 1 Electrical axes, mechanical axes and dipoles in a plate ceramic

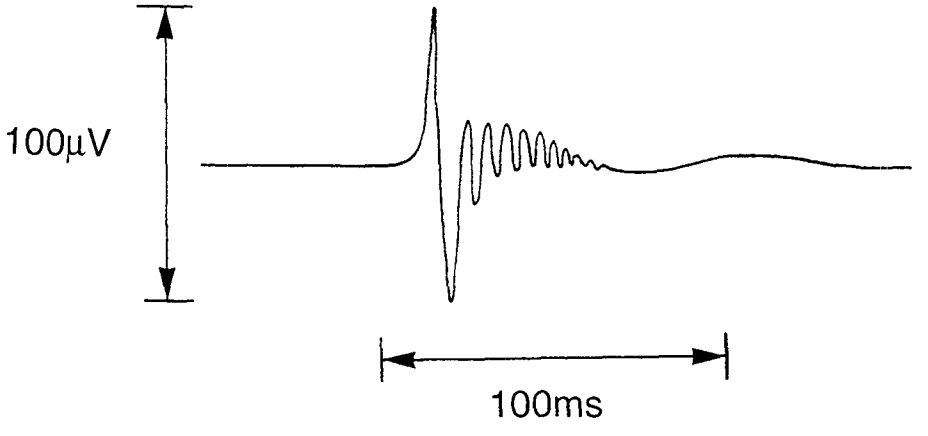

Figure 2 A typical piezoelectric ceramic response signal

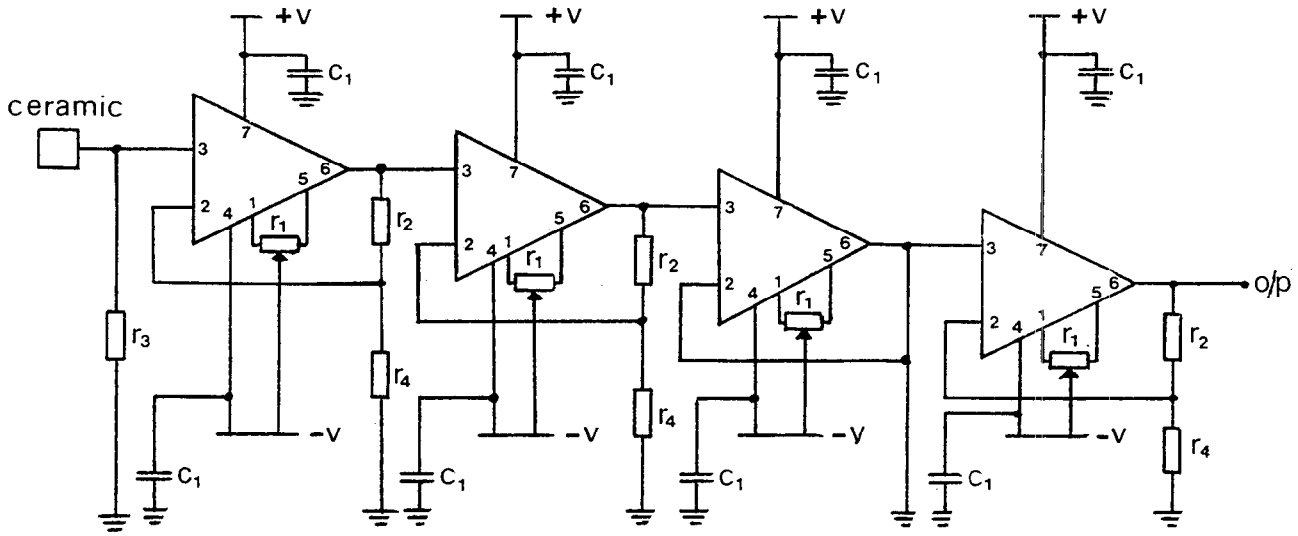

Figure 3 *SSIP* output signal amplification circuit. *(∇ AD711JN; c_1 2.2μF; r_1 10K; r_2 200K; r_3 1K; r_4 9K).*

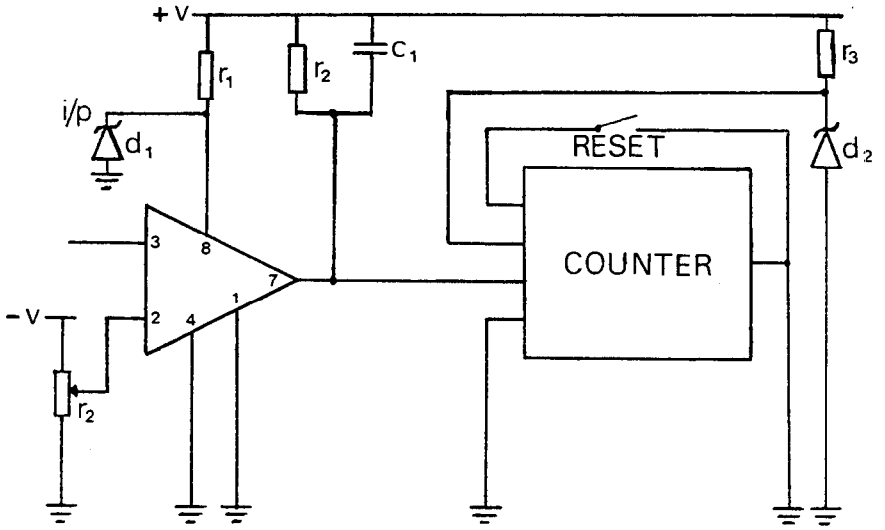

Figure 4 *SSIP* signal counter circuit. *(∇ CMP01CP; c_1 470nF; r_1 5K100; r_2 10K; r_3 5K; d_1 5V1; d_2 3V3).*

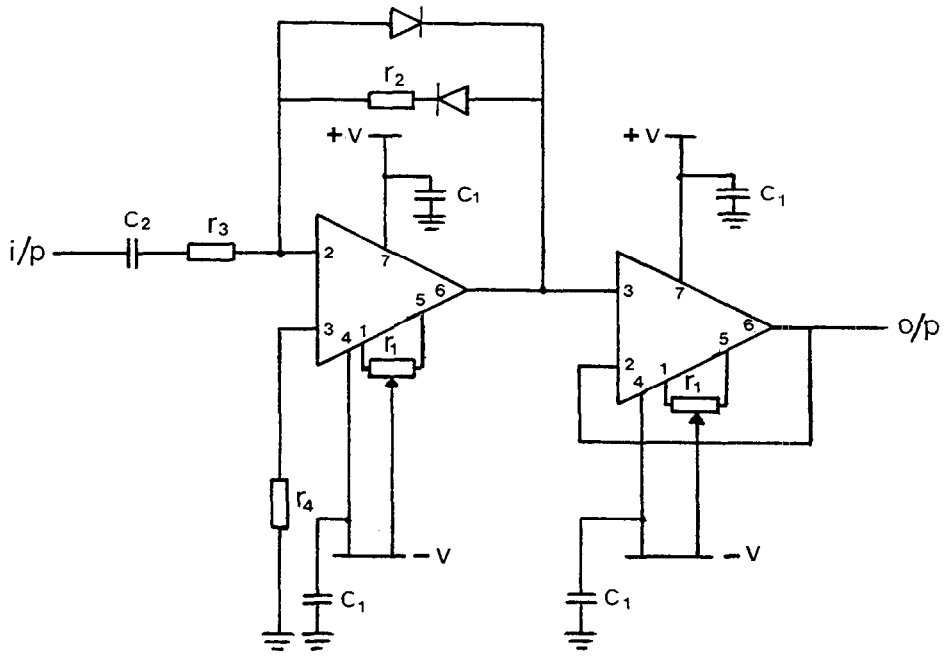

Figure 5 *SSIP* half wave signal rectifier circuit. *(∇ AD711JN; c_1 2.2μF; c_2 10nF; r_1 10K; r_2 56K; r_3 270K; r_4 47K).*

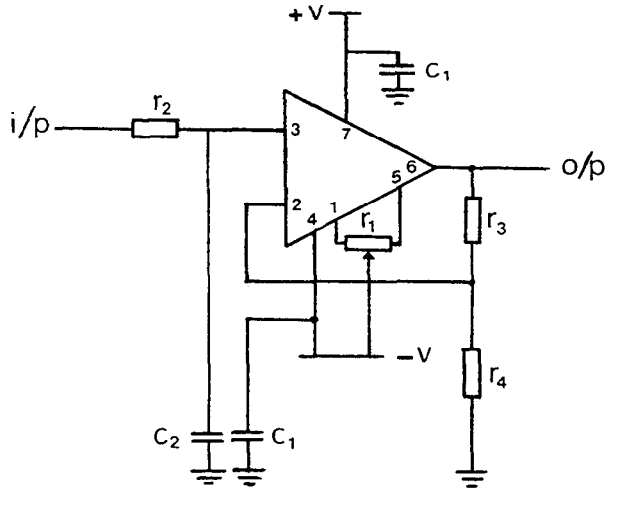

Figure 6 *SSIP* envelope detector circuit. *(∇ AD711JN; c_1 2.2μF; c_2 220nF; r_1 10K; r_2 500K; r_3 270K; r_4 300Ω).*

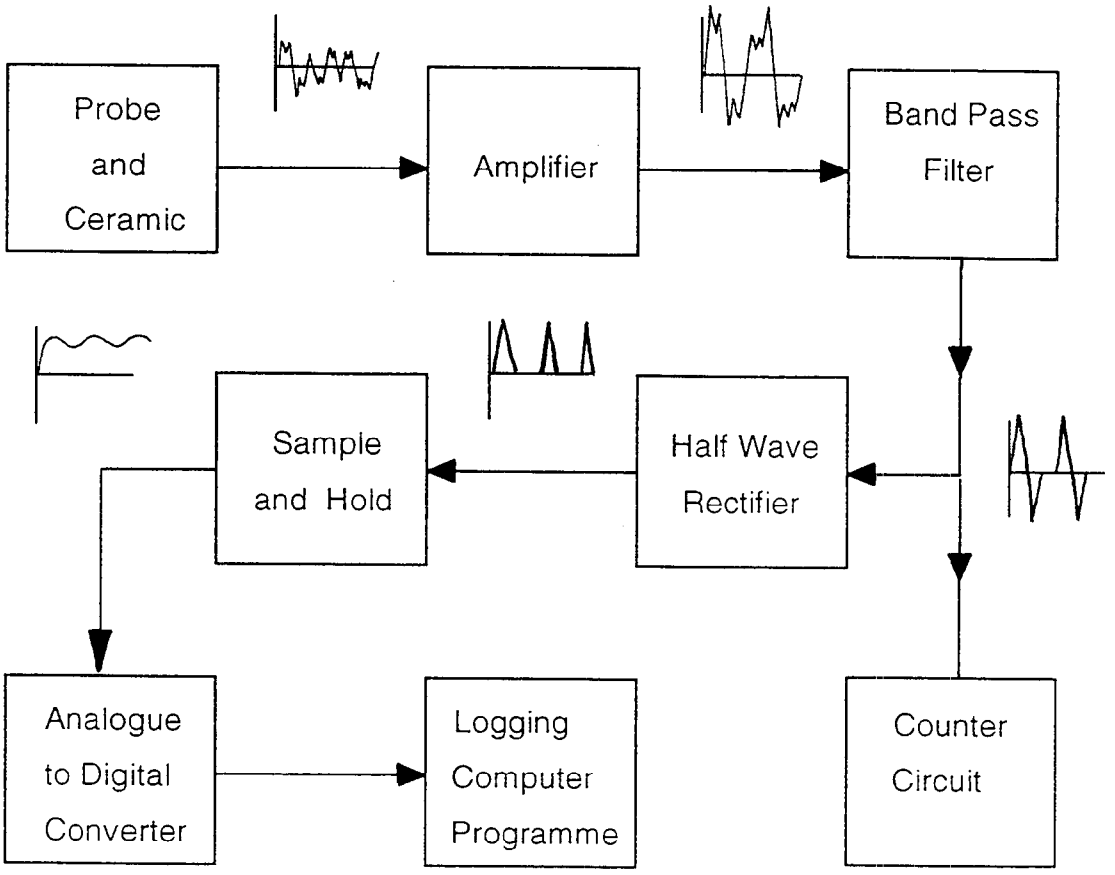

Figure 7 Flow diagram of *SSIP* signal processing electronics and signal shape

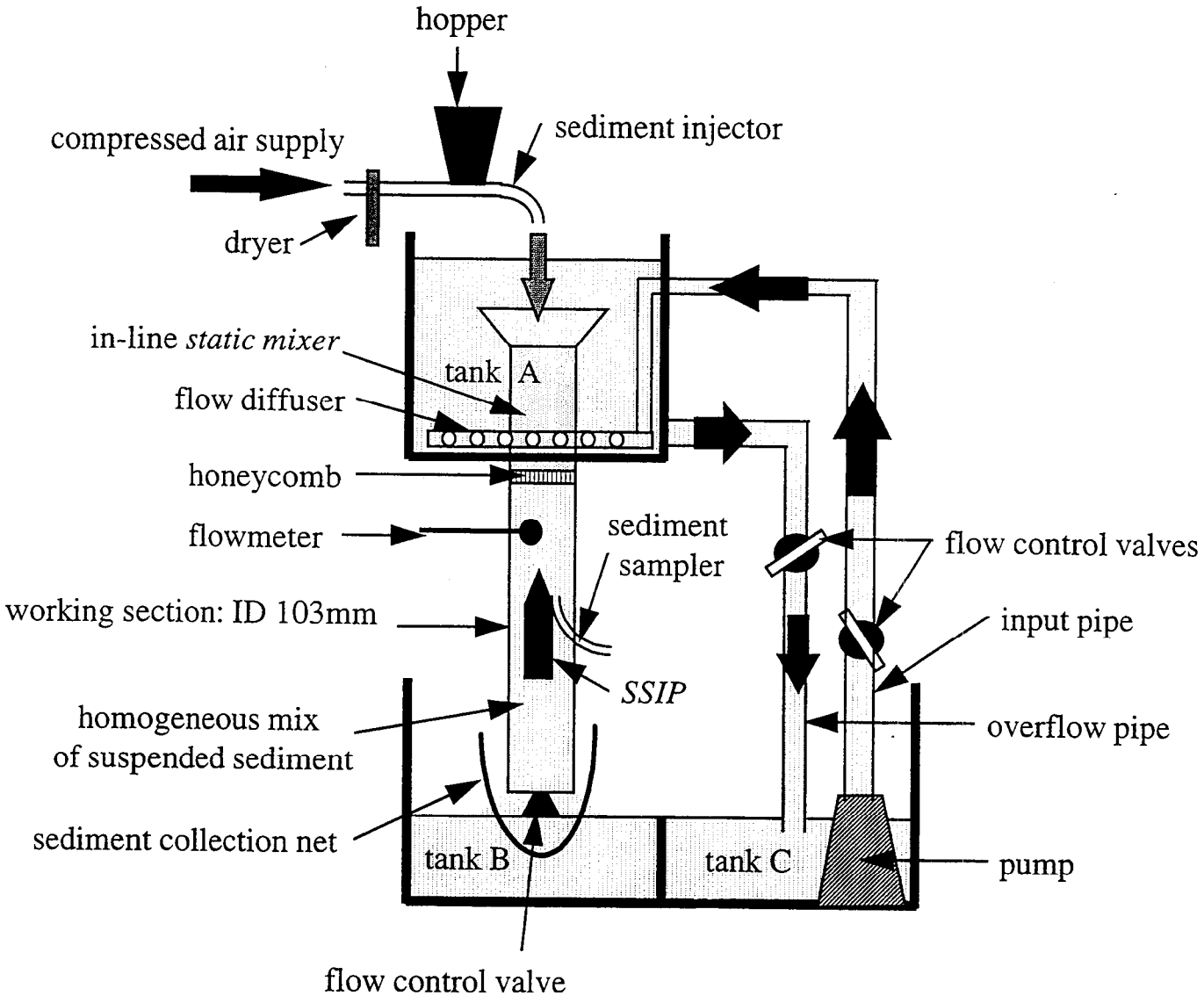

Figure 8 The vertical flume

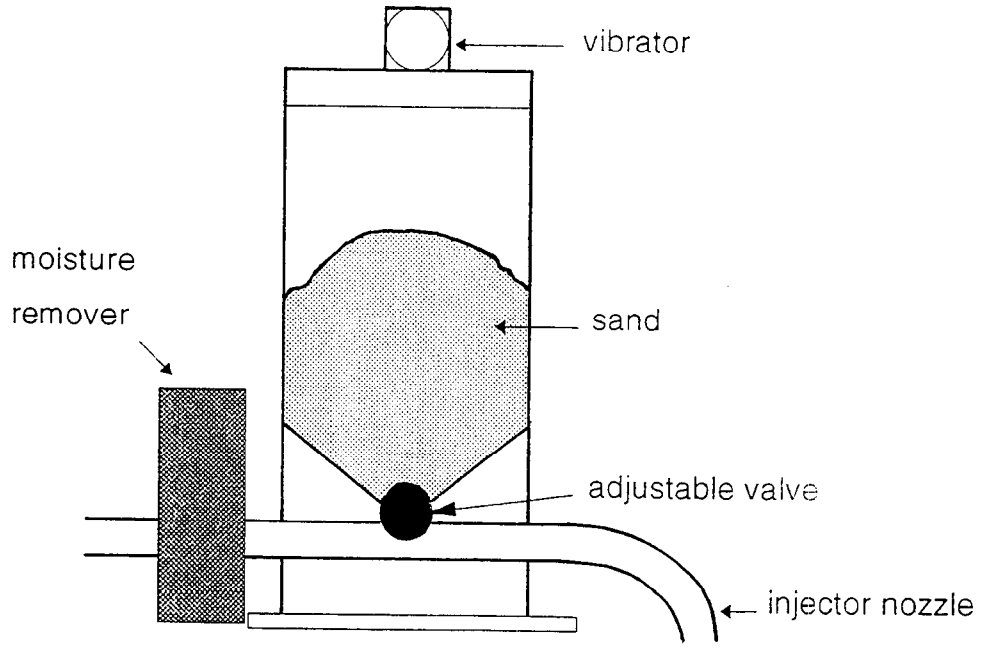

Figure 9 The sand injector

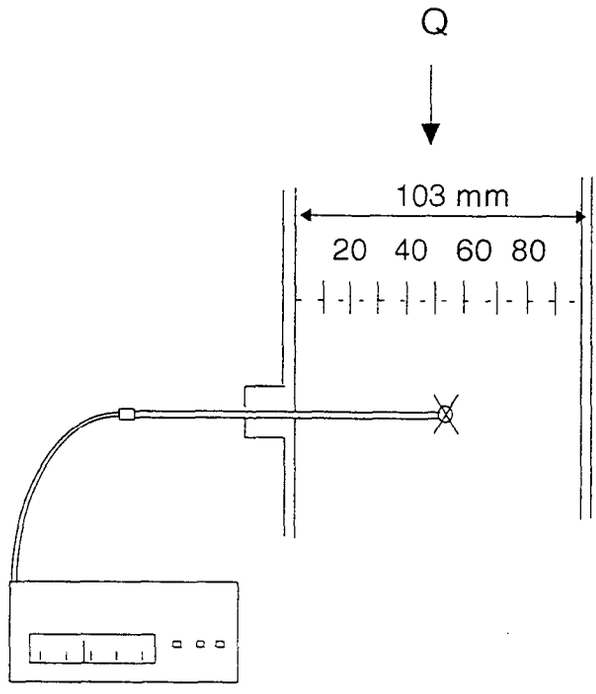

Figure 10 Velocity meter probe positions in the flume

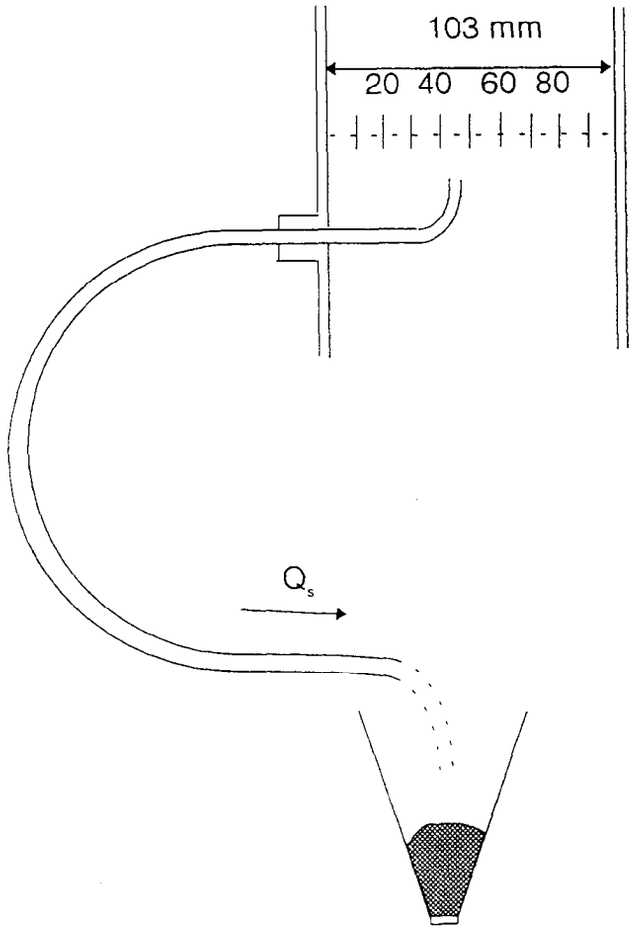

Figure 11 The vertical flume and sampler

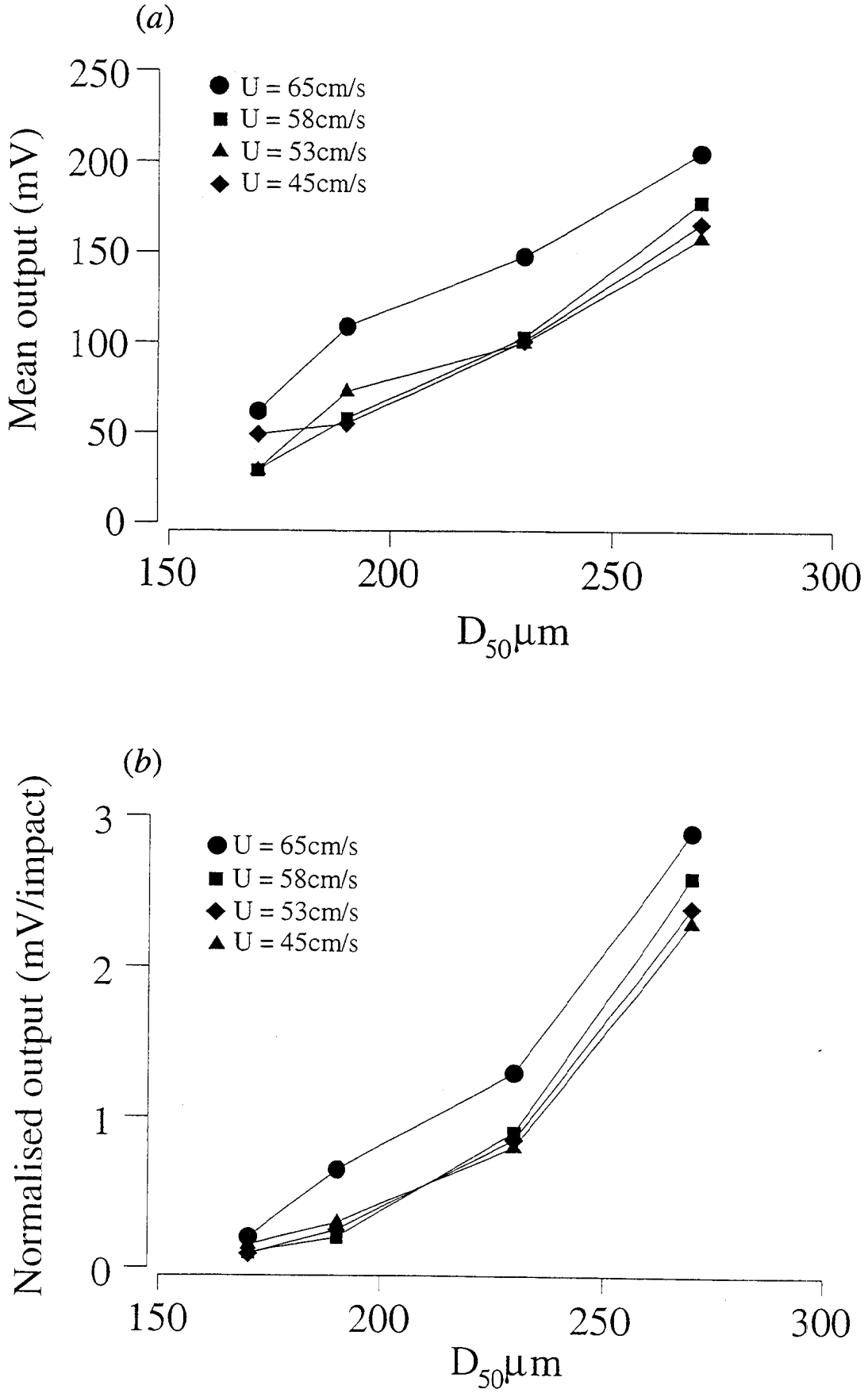

Figure 12 *(a)* Mean output voltage from *SSIP-01* versus D_{50}; and *(b)* Normalised *SSIP-01* output versus D_{50}

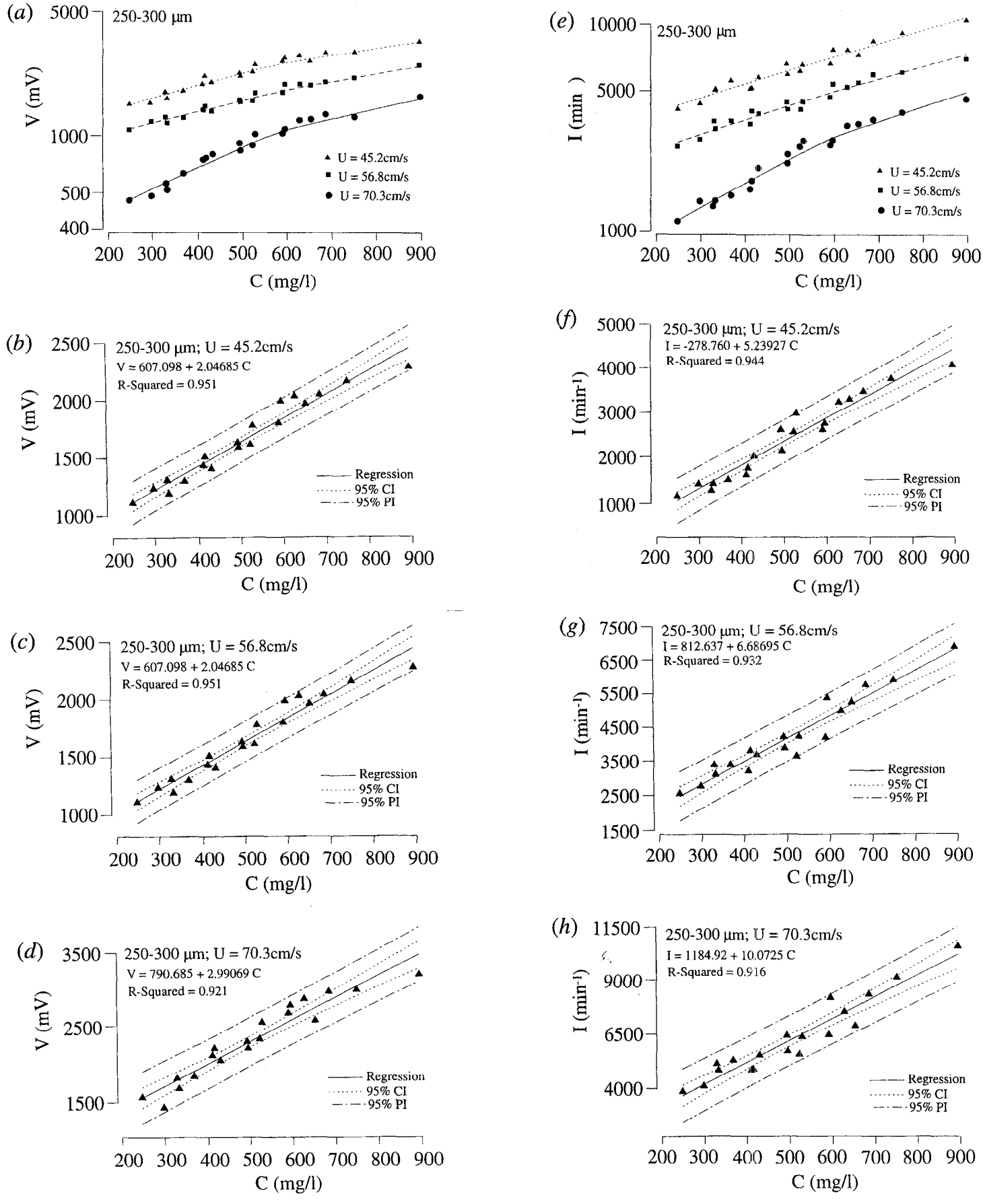

Figure 13 Calibration of *SSIP-02* for 150µm to 180µm sediments

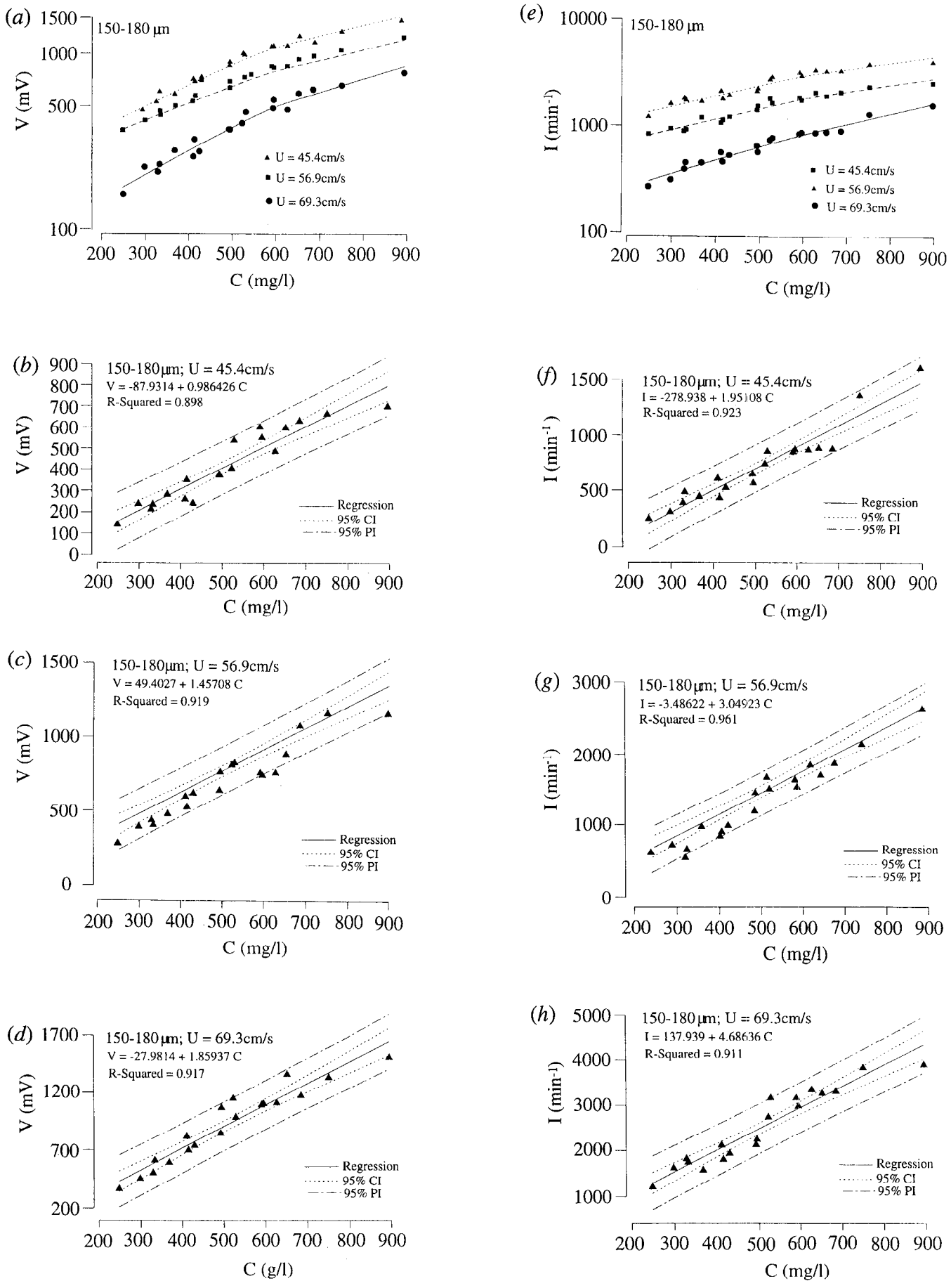

Figure 14 Calibration of *SSIP-02* for 250µm to 300µm sediments

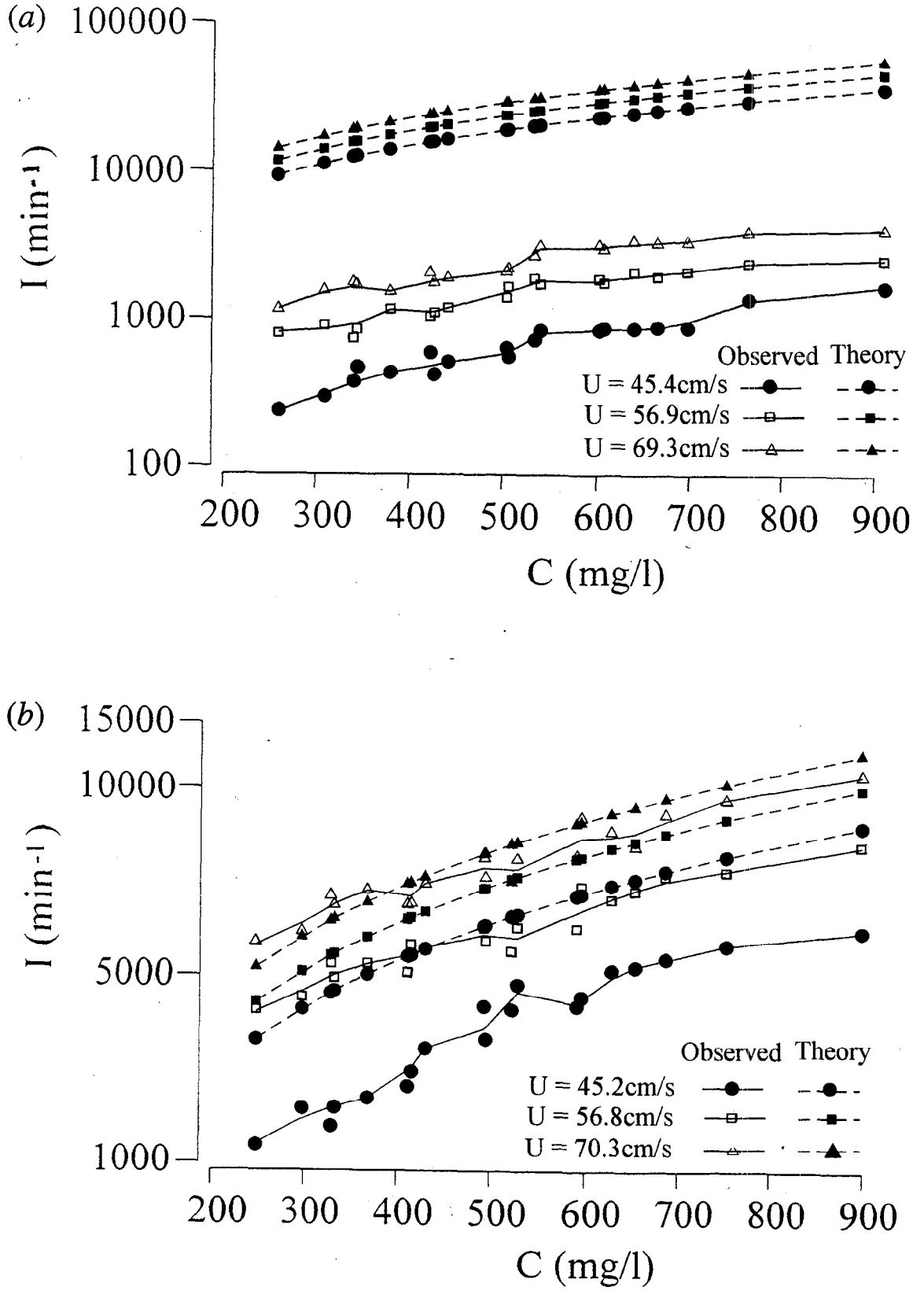

Figure 15 Observed and calculated grain impacts per minute, I, values over the suspended sediment concentration range 250mg/l to 900mg/l for current speeds, U, ≈ 45cm/s, ≈ 57cm/s and ≈ 70 cm/s for : (a) 150μm to 180μm sediment; and (b) 250μm to 300μm sediment.